Title: Succinate dehydrogenase expression and activity: A potential molecular fingerprint with metabolism-rewiring properties and clinical impact in undifferentiated pleomorphic sarcomas

Authors: Miguel Esperança-Martins[1,2,3], Hugo Vasques[3,4], Manuel Sokolov Ravasqueira[5,6], Filipa Santos[7], Filipa Fonseca[4], António Syder Queiroz[1], João Boavida[8], Daniel Martins Jordão[3,9], Joaquim Soares do Brito[3,10], Patrícia Corredeira[2], Marta Martins[2], Ângela Afonso[2], Jorge Antonio López[11], Richard S.P.Huang[12], Cecília Melo Alvim[1,3], Isabel Fernandes[13,14], Dolores López Presa[8], Maria Manuel Lemos[7,8], Brian Van Tine[15,16,17], Alliny C.S. Bastos[15], Sandra Casimiro[2,3], Nuno Abecasis[3,4], Luís Costa[1,2,3], Emanuel Gonçalves[5,6], Iola Duarte[18], Sérgio Dias[2,3]

Affiliations

1 - Medical Oncology Department, Unidade Local de Saúde de Santa Maria; Lisboa, Portugal;

2 - Gulbenkian Institute for Molecular Medicine; Lisboa, Portugal;

3 - Faculdade de Medicina da Universidade de Lisboa, Universidade de Lisboa; Lisboa, Portugal.

4 - General Surgery Department, Instituto Português de Oncologia de Lisboa Francisco Gentil; Lisboa, Portugal.

5 - Instituto de Engenharia de Sistemas e Computadores – Investigação e Desenvolvimento (INESC-ID); Lisboa, Portugal.

6 - Instituto Superior Técnico, Universidade de Lisboa; Lisboa, Portugal.

7 - Pathology Department, Instituto Português de Oncologia de Lisboa Francisco Gentil; Lisboa, Portugal.

8 - Pathology Department, Unidade Local de Saúde de Santa Maria; Lisboa, Portugal.

9 - General Surgery Department, Unidade Local de Saúde de Santa Maria; Lisboa, Portugal.

10 - Orthopedics Department, Unidade Local de Saúde de Santa Maria; Lisboa, Portugal.

11 - F.Hoffmann-LaRoche AG; Basel, Switzerland.

12 - Foundation Medicine Inc; Boston, Massachusetts, United States of America.

13 - Medical Oncology Department, Hospital CUF Descobertas; Lisboa, Portugal.

14 - EpiDoC, CHRC, Nova Medical School, Universidade Nova de Lisboa; Lisboa, Portugal.

15 - Division of Medical Oncology, Washington University in St. Louis; St. Louis, Missouri, United States of America;
16 - Division of Pediatric Hematology/Oncology, St. Louis Children's Hospital, St. Louis, Missouri, United States of America;
17 - Siteman Cancer Center; St. Louis, Missouri, United States of America;
18 - Department of Chemistry, CICECO-Aveiro Institute of Materials, Universidade de Aveiro; Aveiro, Portugal.

* **Corresponding Author** – Miguel Esperança-Martins. E-mail: miguelmemartins@campus.ul.pt.

Abstract

Undifferentiated pleomorphic sarcomas (UPS), leiomyosarcomas (LMS) and liposarcomas (LPS) are the three most common soft tissue sarcoma (STS) subtypes, UPS being the least understood at the molecular level, despite its dismal prognosis. We conducted a multi-omics comparative exploratory analysis of UPS, LMS, and LPS samples in order to identify distinctive molecular traits of UPS that could be targetable.

An RNA-seq analysis of formalin-fixed paraffin-embedded (FFPE) samples of UPS, high-grade LMS, and dedifferentiated LPS (DDLPS) revealed a transcriptomic similarity between UPS and high-grade LMS. UPS showed increased expression of succinate dehydrogenase (SDH) subunit encoding genes. Over expression of *SDHB* was significantly associated with shorter overall survival (OS) and OS from metastasis date in UPS. The differential gene expression findings were validated using the TCGA-SARC dataset.

The protein expression of SDHB was assessed by immunohistochemistry using the same FFPE samples. UPS and LMS showed higher SDHB protein levels than DDLPS and an elevated SDHB protein abundance.

An exploratory metabolomic analysis using ^{1}H NMR on fresh tumor samples of UPS, LMS and LPS revealed significant differences in 10 metabolites across subtypes, with UPS showing higher levels of amino acids, uracil, and carnosine. Moreover, the succinate-to-fumarate ratio was significantly higher in UPS, suggesting possible functional impairment of SDH enzymatic activity, potentially due to post-translational modifications, altered assembly of SDH subunits, or imbalanced TCA flux.

These findings highlight distinct metabolic vulnerabilities in UPS and warrant validation in larger, molecularly defined cohorts to assess their potential as diagnostic biomarkers or therapeutic targets.

Keywords: Undifferentiated Pleomorphic Sarcomas, Multi-omics, RNA-seq, Immunohistochemistry, ^{1}H NMR, Succinate Dehydrogenase.

Introduction

Soft tissue sarcomas (STS)' rarity (1% of all adult malignancies and 15% of non-hematologic childhood neoplasms [1]) and heterogeneity (classification in 50 to 150 histopathological subtypes [2]) promotes an unpropitious conceptual framing for pre-clinical studies and for early and late-phase clinical trials development. Recognition of subtype-characteristic molecular traits, identification of specific targets for precision treatment approaches and the discovery, development and use of new pharmacological agents or platforms has occurred at a particularly slow pace in sarcomas. The knowledge of the molecular landscape of STS keeps being scarce and the dismal prognosis of a non-despicable proportion of early-stage STS and of the great majority of late-stage STS remains nearly unmodified in the last decades.

Among STS, undifferentiated pleomorphic sarcomas (UPS) and L-type sarcomas (leiomyosarcomas (LMS) and lipossarcomas (LPS)) constitute the three most common histopathological subtypes [3]. UPS remains the worst characterized in what molecular profile and molecular distinctive traits is concerned. The potential impact of portraying UPS molecular landscape is significant since UPS account for 17% of all STS [4], being high-grade, aggressive STS with dismal 5- and 10-year overall survival rates (OS) (60 and 48%, respectively [5]) and whose local and distant recurrence rates are non-despicable (14.1 and 7.8%, respectively [6]).

The definition of UPS has been dynamic throughout times. The constituting cells of STS nowadays classified as UPS were initially thought to have prototypical characteristics of histiocytes, which led to their initial classification as malignant fibrous histiocytoma [7,8,9]. These cells were then considered to display fibroblastic phenotypic characteristics when examined with new analytical modalities [7,10-14]. Nowadays, UPS are eminently a diagnosis of exclusion [7], which relies on the sequential exclusion of a non-mesenchymal neoplasm, another well-classified STS, a component of a dedifferentiated sarcoma, and a pleomorphic sarcoma with a specific line of differentiation [7].

The true molecular and cellular origin of UPS is still not clear. Some past reports outlined similarities between UPS and LMS, suggesting that they share common oncogenic pathways and may correspond to different stages of the same oncologic entity [15-17]. In parallel, the recognition of a specific line of differentiation within a UPS tissue through cytoarchitectural evaluation and immunohistochemical staining is relevant since pleomorphic STS with myogenic differentiation seem to be more clinically aggressive than those without myogenic differentiation [7,15,18,19]. However, the practical

feasibility and the overall sensitivity of the attribution of a myogenic differentiation pattern to an UPS based on histologic and immunohistochemical data is relatively low [7].

Molecular profiling studies, namely multi-omics studies, are therefore essential to highlight specific molecular traits of UPS and to underpin the differences between UPS and pleomorphic/high-grade LMS and between UPS and dedifferentiated LPS (DDLPS). The inclusion of metabolomic studies in multi-omics approaches may provide clues with a superlative biological value. Metabolic profiles, in a broad perspective, and metabolites, in a precise sense, are end-products of biochemical interactions and are the closest biochemical representation of the phenotype [20,21]. Metabolites themselves are small molecules with a pleiotropic nature [22,23,24].

Metabolomic studies, either as a single-omics approach or as part of a multi-omics strategy, feed the scarce body of knowledge regarding the metabolic profiles and signatures of STS [25]. Indeed, the number of metabolomic studies focused on STS is particularly short, using small numbers of heterogenous samples of a limited range of STS subtypes. Studies that employed mass spectrometry used sample sets whose composition ranged from 5 human formalin-fixed and paraffin-embedded (FFPE) STS samples [26] to fresh tissue samples of autochthonous STS murine models [27]. The only study that employed mass spectrometry imaging used fresh frozen tissue samples of high-grade STS obtained from 33 human patients [28]. The heterogeneity of the constitution of the sample sets that were used in the short number of Nuclear Magnetic Resonance (NMR) Spectroscopy studies of STS is striking, with different types of cell lines and of normal and tumor tissue being used for a plethora of *in vitro*, *in vivo* and *ex vivo* studies [29-41]. A few of these studies employed human tissue samples obtained from 9-36 patients with a wide variety of STS [29-41].

In this study, we portrayed patterns of gene expression, in particular of metabolism-related genes and pathways, and studied their correlation with clinical endpoints using UPS, high-grade LMS and DDLPS samples. Then, we validated the uncovered patterns of expression of a metabolism-related gene at the protein level in STS tissue samples using immunohistochemistry. Finally, we performed an exploratory, unbiased characterization of the metabolome of UPS, LMS and LPS cases to identify key metabolites and main metabolic pathways whose activity could be characteristic of each of these STS subtypes. Together, our exploratory approach generated novel and innovative data suggesting the existence of relevant metabolic and related transcriptomic differences between STS subtypes, contributing towards the identification of putative specific novel therapeutic targets in these rare cancers.

Material and Methods

Gene expression analysis

Tissue cohort

This cohort comprised 102 formalin-fixed paraffin-embedded (FFPE) tumor samples, obtained from 101 patients diagnosed with a high-grade (grade 3) STS (25 with a DDLPS, 25 with a high-grade LMS, and 51 with an UPS), and has been previously characterized in terms of demographic, pathological, surgical, and systemic treatment specificities [42].

DNA and RNA sequencing

This set of FFPE samples was analyzed with FoundationOne®CDx (F1CDx) for DNA Sequencing (DNA-seq) [43] and with FoundationOne®RNA (F1RNA) for RNA sequencing (RNA-seq) (gene expression data for F1RNA is research use only (RUO)) [44].

Testing was performed in a Clinical Laboratory Improvement Amendments (CLIA)-certified, College of American Pathologists (CAP)-accredited, New York State-approved laboratory (Foundation Medicine, Inc., Cambridge, MA, USA).

DNA and RNA were simultaneously co-extracted and isolated from FFPE samples, as previously described [42].

Quality Control

Out of 102 STS samples (26 DDLPS, 25 LMS and 51 UPS), 79 samples passed F1CDx quality control, and 75 samples passed F1RNA quality control. Of note, the samples that did not pass F1RNA quality control tended to be archival samples with a median age of 4.7 years. One additional sample was excluded from the RNA-seq expression analysis after being identified as an outlier using principal component analysis (PCA). A total of 74 samples (16 DDLPS, 15 LMS and 43 UPS) were therefore considered for downstream expression analysis.

RNA-seq-based differential gene expression analysis

The computational analyses were performed using R (v4.4.0). RNA-seq data from these 74 samples was filtered for expression using the edgeR (v4.2.1) [45] filterByExpression method to remove lowly expressed genes, followed by Voom normalization. Differential

gene expression (DGE) analysis was then conducted between histopathological subtypes using the limma package [46] (v3.60.4) and p-values were adjusted for multiple hypothesis testing using Benjamini-Hochberg False Discovery Rate (BH-FDR). Differentially expressed genes (DEGs) were identified using an adjusted p-value threshold of ≤ 0.05. The concordance between metabolic pathways and genes included in F1RNA, was identified using the Kyoto Encyclopedia of Genes and Genome pathways [47].

Assessment of differentially expressed genes' clinical significance (study cohort)

Survival analysis was performed using survival package (v3.7.0) [48] for different clinical endpoints, Overall Survival (OS), Metastasis-Free Survival (MFS), Recurrence-Free Survival (RFS), Progression-Free Survival (PFS), and OS from Metastasis Date. Survival analysis was performed within and between each histopathological subtype and for each gene baited for expression included in F1RNA, classifying samples as highly or lowly expressed for a given gene, based on whether gene expression levels were above or below the mean expression of the gene, and a log rank test p-value was obtained for each gene. Over-representation analysis [49] (ORA) was performed for each DGE comparison, stratified by direction of expression (over expressed and under expressed genes). Additionally, ORA was conducted on gene sets identified as significant in the survival analysis (log-rank p-value < 0.05), separately evaluating genes for which high expression was associated with favorable prognosis and those for which high expression was associated with poor prognosis.

External validation using TCGA-SARC (independent cohort)

The TCGA-SARC [50] dataset was used as an independent validation cohort and filtered to include only samples classified as UPS, LMS, and DDLPS, based on the revised histopathological classification. Identical RNA-seq processing steps were applied, including filtering, normalization, and differential gene expression analysis using limma. The same survival analysis methodology was also applied, where each gene was independently assessed for prognostic significance using the log-rank test to compute p-values. ORA was also performed in the TCGA cohort for each DGE comparison, again stratified by direction of expression (over expressed and under expressed). Furthermore, ORA was carried out on gene sets identified as significant in the TCGA survival analysis (log-rank p-value < 0.05), analyzing separately the genes for which high expression was

associated with improved prognosis and those for which high expression was associated with worse prognosis.

To assess whether soft tissue sarcomas from the TCGA-SARC cohort were comparable to those in the study cohort given the histopathological subtypes, we evaluated whether the direction of expression changes between subtypes was consistent across cohorts. For each pairwise comparison (LMS vs DDLPS, UPS vs LMS, UPS vs DDLPS), we identified genes with an adjusted p-value < 0.05 in both cohorts and intersected these sets. Within the overlapping gene set, we then compared the direction of expression changes by analyzing log fold-change (logFC) values to determine whether genes were consistently over expressed ($\text{logFC} > 0$) or under expressed ($\text{logFC} < 0$) in both datasets. Statistical significance of the directional concordance was assessed using a hypergeometric test. In addition to DGE concordance, we investigated the consistency of survival associations. Focusing on the UPS subtype, we selected genes significantly associated with overall survival (OS), defined by a log-rank test p-value < 0.05, in each cohort. For each gene, we determined whether higher expression was associated with a favorable or unfavorable prognosis. We then intersected the sets of significant genes from the study cohort and TCGA and compared the directionality of their survival associations—i.e., whether high expression was consistently linked to either improved or worsened survival across datasets. This concordance was also evaluated using a hypergeometric test, following the same logic as in the DGE comparison.

Immunohistochemical evaluation of SDHB protein levels

Each of the 102 FFPE tumor samples was reviewed by a pathologist with experience in soft tissue pathology. All cases were fixed in 10% formalin. Immunohistochemical analysis was performed on deparaffinized sections using a standard avidin–biotin–peroxidase complex method in an automated platform (BenchMark ULTRA, Ventana medical system, Tucson, AZ, USA). FFPE blocks were qualitatively analyzed for the expression of a rabbit monoclonal antibody SDHB (clone: EP288; ref. MAD-000739QD; Vitro Master Diagnóstica™, Granada, Spain). External positive and negative controls using sections of gastrointestinal stromal tumors were immunostained in parallel with all cases. Two pathologists blinded to all clinical, pathological and molecular data scored immunoreactivity. Definite granular staining in the cytoplasm of tumor cells was considered positive. A three-tier score was used to identify variations in immunostaining and cases were grouped as: score 1 - focal and weak staining (<10% of cells, 1); score

2 - diffuse and intermediate staining (10-90% of cells, 2); score 3 – diffuse and strong staining (>90% of cells, 3). Additionally, cases lacking unequivocal cytoplasmic granular staining were considered negative and cases lacking a definite positive internal control were considered non-informative.

Nuclear Magnetic Resonance (NMR) Metabolomics

Tissue cohort

The cohort included STS cases with indication for surgery, collected between 2021 and 2023 in two Portuguese sarcoma reference centers, Instituto Português de Oncologia de Lisboa Francisco Gentil (IPOLFG) and Unidade Local de Saúde de Santa Maria (ULSSM). The composition of the cohort intended to represent the heterogeneity of the universe of sarcoma cases that are operated, and for which the surgical obtention, processing and storage of fresh frozen normal and tumor tissue is feasible in these two sarcoma reference centers.

Samples included 12 fresh normal tissue and 15 fresh tumor tissue samples surgically obtained from 16 patients. The set of 15 fresh tumor tissue samples comprised three samples of UPS, three samples of LMS, two samples of LPS - one of DDLPS and one of myxoid liposarcoma (MLPS) -, one sample of dermatofibrosarcoma protuberans (DFSP), one sample of solitary fibrous tumor (SFT), one sample of synovial sarcoma (SS), one sample of chondrosarcoma (CS), one sample of clear-cell sarcoma-like tumor of the gastrointestinal tract (CCSLGT), one sample of endometrial stromal sarcoma (ESS), and one sample of adamantinoma (ADM). All histopathological diagnoses were confirmed by a dedicated sarcoma pathologist, ensuring diagnostic consistency and quality control across the dataset.

Comprehensive clinical data were obtained for all these patients through review of institutional medical records at both participating hospitals. This was supplemented with information from the national electronic health record system. Variables collected included patient demographics, tumor characteristics (histological subtype, grade, location), treatment modalities (surgery, radiotherapy, systemic therapy), surgical margins, and oncological follow-up.

An anonymized research database was developed specifically for this study, and clinical follow-up was closed on April 21, 2025.

Metabolite extraction from fresh tissue

Fresh normal and tumor tissue samples were first macerated using an agate mortar and pestle under liquid nitrogen and stored at –80 °C until further usage. For metabolite extraction, 650 μL of cold methanol 80%, 520 μL of cold chloroform, and 260 μL of cold Milli-Q water were sequentially added per 50 mg of tissue. Each solvent addition was followed by 1 minute of vortexing to ensure proper mixing. After the final addition of water and vortexing, samples were incubated at 4 °C for 20 minutes and then centrifuged at 3000 ×g for 10 minutes. A 500 μL aliquot of the resulting upper aqueous phase was collected, dried in a speed vacuum concentrator (Centrivap, model 73100, Labconco, Kansas City, MO, USA), and stored at –80 °C until further analysis.

<u>^{1}H NMR data acquisition and analysis</u>

For NMR analysis, the dried samples were dissolved in 200 µL of deuterated phosphate buffer (PBS,100 mM, pH 7.4) containing 0.1 mM 3-(trimethylsilyl) propanoic acid (TSP-d4), and approximately 180 µL of each sample were transferred to 3 mm NMR tubes. All samples were analyzed in a Bruker Avance III HD 500 NMR, operating at 500.13 MHz for 1H observation, at 298 K, using a 5 mm TXI probe. Standard 1D 1H spectra with water presaturation (pulse program 'noesypr1d' from Bruker library) were acquired with 32 k points, 7002.80 Hz spectral width, a 2 s relaxation delay, and 512 scans. All spectra were processed in TopSpin 4.0.3 (Bruker BioSpin, Rheinstetten, Germany), using cosine multiplication (ssb 2), zero-filling to 64 k data points, manual phasing, baseline correction, and calibration to the TSP-d4 signal (0 ppm). 1H-1H TOCSY and J-resolved spectra were also acquired for selected samples. Metabolite assignment was based on matching 1D and 2D spectral information to reference spectra available in Chenomx (Edmonton, Canada) and BBIOREFCODE-2–0–0 (Bruker Biospin, Rheinstetten, Germany).

To provide a relative quantitative measurement of metabolic variations, spectral integration and total area normalization of selected signals were carried out in Amix-Viewer 3.9.15 (Bruker Biospin, Rheinstetten, Germany).

All statistical analyses were performed using GraphPad Prism version 8 (GraphPad Software Inc., CA, USA). Data normality was assessed through the Shapiro-Wilk test. For comparisons involving three independent groups, one-way ANOVA followed by Tukey's multiple comparison test was applied when data met parametric assumptions; otherwise, the non-parametric Kruskal–Wallis test followed by Dunn's post hoc test was used. Comparisons between two independent groups were conducted using the

unpaired Student's t-test with Welch's correction, or the Mann–Whitney test for non-normally distributed data. Statistical significance was considered at a p-value < 0.05.

Results

Gene expression analysis suggests molecular similarity between UPS and high-grade LMS, reveals the over expression of SDH subunit encoding genes in UPS, and a correlation between *SDHB* over expression and clinical endpoints in UPS

Characterization of the patients whose FFPE samples were analyzed

An extensive description of the demographic, pathological, surgical and systemic treatment specificities of the 101 patients whose 102 FFPE tumor samples were used for this gene expression analysis has been provided [42].

Differential gene expression analysis suggests a closer molecular resemblance between UPS and high-grade LMS

Differential gene expression analysis revealed an UPS gene expression pattern more similar to high-grade LMS than to DDLPS (Supplementary Figure 1).

This finding is supported by the lower number of differentially expressed genes (DEGs) between UPS and high-grade LMS (67 DEGs; Supplementary Table 1) compared to UPS and DDLPS (241 DEGs; Supplementary Table 2), as well as by the smaller magnitude of differential gene expression, with a mean log fold change (logFC) of 0.009 for UPS vs. high-grade LMS and 0.01 for UPS vs. DDLPS.

Genes involved in metabolic processes are differentially expressed in UPS

To identify molecular features unique to UPS, a deeper analysis of differentially expressed genes and pathways between UPS and high-grade LMS, and between UPS and DDLPS was performed. Notably, several metabolism-related genes and pathways emerged. Although the F1RNA expression gene set was not specifically designed to focus on metabolism-related genes and metabolic pathways, containing only 84 metabolism-related genes out of 1,519 and covering 22 metabolic pathways, each with a limited number of genes (Supplementary Table 3 and Supplementary Figure 2), a targeted analysis focusing solely on these metabolic components was conducted (Supplementary Figure 3 and Supplementary Table 4).

Three genes involved in the tricarboxylic acid (TCA) cycle and in oxidative phosphorylation (OXPHOS) (*SDHB*, *SDHC* and *SDHD*), and one gene associated with

arachidonic acid metabolism (*ALOX12*) were found to be differentially expressed between UPS and high-grade LMS (Supplementary Figure 4 and Supplementary Table 4). A similar comparison between UPS and DDLPS identified a larger number of differentially expressed metabolic genes and pathways. Notably, the only overlapping metabolic changes between both comparisons were the differential expression of the same three TCA cycle genes, three OXPHOS genes, and one arachidonic acid metabolism gene.

SDHB, *SDHC* and *SDHD* are over expressed in UPS relatively to high-grade LMS and to DDLPS

The overexpression of *SDHB*, *SDHC*, and *SDHD* in UPS (either vs. high-grade LMS and also vs. DDLPS) (Supplementary Figure 3) aligns with the broader metabolic signature distinguishing UPS from both high-grade LMS and DDLPS. These genes encode subunits of the succinate dehydrogenase (SDH) complex, a mitochondrial enzyme that functions at the interface of the TCA cycle and the electron transport chain, linking these two metabolic systems (TCA cycle and OXPHOS).

Differential expression analysis using the Limma-Voom method confirmed that *SDHB*, *SDHC*, and *SDHD* were significantly overexpressed in UPS relative to both high-grade LMS and DDLPS, as shown in Figure 1. All three genes showed statistically significant *p-values* and positive log fold-change (logFC) values, reinforcing their potential role as defining metabolic markers of UPS.

SDHB over expression is significantly correlated with a shorter OS and a shorter OS from metastasis date in UPS

The correlation between the relative over expression of *SDHB*, *SDHC* and *SDHD* and clinical outcomes, including overall survival (OS), progression-free survival (PFS), recurrence-free survival (RFS), metastasis-free survival (MFS) and OS from metastasis date, were assessed both in the specific UPS subgroup and also in the overall cohort population.

In UPS, *SDHB* over expression was significantly correlated with shorter OS, both in a survival analysis using the Kaplan-Meier method (KMM) (*p-value* <0.05) (Figure 2a) and in a survival analysis using a Cox Proportional Hazards Model (CPHM) (*p-value* <0.05) (Figure 2b). Additionally, it also showed a statistically significant correlation with shorter OS from metastasis date, both in a survival analysis using the KMM (*p-value* <0.01) (Figure 2c) and in a survival analysis using a CPHM (*p-value* <0.05) (Figure 2d). Moreover, for this specific UPS population, *SDHB* over expression did not show a statistically significant correlation with either MFS, RFS, and PFS, but was consistently

associated with a trend towards shorter MFS, RFS and PFS (Supplementary Figure 5). In contrast, *SDHC* and *SDHD* over expression did not show a statistically significant correlation with OS and any of the above-mentioned clinical endpoints (Supplementary Figures 6 and 7).

Interestingly, in the whole cohort population, *SDHB, SDHC and SDHD* over expression did not show correlation with OS in any of the analysis performed or with any of the other evaluated clinical endpoints (Supplementary Figure 8 to 11).

Among the SDH genes, *SDHB* was the only one whose overexpression showed a significant correlation with both overall survival (OS) and OS from the date of metastasis in the UPS population. To further assess the robustness of this association, *SDHB* expression was analyzed as a continuous variable. Under these conditions, the correlation signal persisted, but the statistical significance was lost for both endpoints (Supplementary Figures 12 and 13).

<u>TCGA-SARC validation confirms the closer molecular similarity between UPS and high-grade LMS and highlights UPS-specific metabolic, immune, and DNA damage repair pathway signatures</u>

To validate the closer molecular similarity between UPS and high-grade LMS observed in the RNA-seq analysis of the study cohort, gene expression data of UPS, high-grade LMS and DDLPS samples included in the TCGA-SARC dataset were analyzed.

As shown in the Volcano Plots (Supplementary Figure 14) and detailed in Supplementary Tables 5 and 6, the number of DEG between UPS and high-grade LMS was markedly lower than between UPS and DDLPS. This finding mirrors the gene expression patterns identified in the study cohort, further supporting the closer molecular resemblance between UPS and high-grade LMS.

Building on the gene expression analysis, differential pathway expression was also assessed using the TCGA-SARC cohort to validate the differential over expression of specific metabolic pathways (TCA cycle and OXPHOS) observed in the study cohort. The Gene Signature Enrichment Analysis (GSEA) and the subsequent differential pathway expression analysis confirmed the upregulation of several metabolic pathways in UPS (with OXPHOS and pyrimidine metabolism being part of the 15 most significantly upregulated pathways in UPS relatively to high-grade LMS (Supplementary Figure 15)) and revealed additional differences involving immune response and DNA repair pathways. Indeed, pathways related to immune activation, such as Graft-versus-Host Disease and Antigen Processing and Presentation, and DNA damage repair mechanisms, including Homologous Recombination, Nucleotide Excision Repair, and Base Excision Repair, were significantly enriched in UPS (Supplementary Figure 15).

A broader analysis of the full spectrum of differentially expressed metabolism-related pathways between UPS and LMS samples reinforced the over expression of multiple components of mitochondrial OXPHOS in UPS, including the respiratory chain complex, complex II (SDH), the electron transport chain, and ATP synthesis-related processes. The TCA cycle was also found to be upregulated in UPS relative to LMS. Comparative analyses involving LMS and DDLPS, as well as UPS and DDLPS, are also provided in Supplementary Figure 16.

Together, these findings reinforce the molecular resemblance between UPS and high-grade LMS, while underscoring the distinct metabolic reprogramming and heightened immune and DNA repair activity that uniquely characterize UPS.

<u>TCGA-SARC validates the differential expression of SDH-encoding genes between UPS, high-grade LMS and DDLPS: SDHA and SDHB are over expressed in UPS relatively to the other STS histotypes in this independent cohort</u>

To assess if TCGA-SARC can be used, with methodological adequacy and robustness, to externally validate the differential gene expression patterns of SDH-encoding genes that were found for specific STS histotypes in our study cohort, we evaluated whether the directionality of gene expression changes (over or under expression) was conserved across both datasets. For each pairwise comparison (UPS vs. LMS, UPS vs. DDLPS, LMS vs. DDLPS), we identified genes significantly differentially expressed (adjusted *p-value* < 0.05) in both cohorts and compared their logFC values to determine directional concordance (over expressed and under expressed) (Supplementary Figures 17, 18 and 19). This directional agreement was statistically significant in all comparisons based on Chi-square tests (UPS vs LMS: *p-value* < 0.01; UPS vs DDLPS: *p-value* < 0.01; LMS vs DDLPS: *p-value* <0.01) (Supplementary Figure 20).

Next, we performed similar differential gene expression analyses comparing UPS with high-grade LMS and with DDLPS samples from the TCGA-SARC cohort. In both comparisons, *SDHA* and *SDHB* emerged as commonly differentially expressed genes. Notably, the differential expression of *SDHB* between UPS and both high-grade LMS and DDLPS was consistently observed in both the study cohort and the independent TCGA-SARC dataset.

Limma-Voom differential expression of *SDHA*, *SDHB*, *SDHC* and *SDHD* was performed for UPS vs. high-grade LMS vs. DDLPS (Figure 3). *SDHA* differential expression between UPS and high-grade LMS is statistically significant (adjusted *p-value* <0.05), being over expressed in UPS (logFC 0.593). Additionally, its differential expression between UPS and DDLPS is also statistically significant (adjusted *p-value* <0.05), also being over expressed in UPS (logFC 0.535). *SDHB* differential expression between UPS

and high-grade LMS is statistically significant (adjusted *p-value* <0.01), being over expressed in UPS (logFC 0.501). Moreover, its differential expression between UPS and DDLPS is also statistically significant (adjusted *p-value* <0.01), also being over expressed in UPS (logFC 0.479). These results highlight consistent overexpression of key SDH subunit genes, particularly *SDHA* and *SDHB*, as a molecular feature of UPS.

<u>TCGA-SARC cannot be used to externally validate the survival impact of the differential expression of SDH-encoding genes in the STS histotypes and specifically in UPS</u>

We attempted to validate the statistically significant correlation that was found between *SDHB* over expression and a shorter OS for UPS in the study cohort.

In addition to evaluating the differential gene expression concordance between our study cohort and TCGA-SARC, we also examined whether the direction of the association between gene expression and OS was consistent across both cohorts. For this purpose, we identified genes whose expression was significantly associated with OS (log-rank test *p-value* < 0.05) in each cohort and determined whether their high expression predicted better or worse prognosis. The overlap of significant genes was then used to evaluate whether the direction of survival association was conserved.

For the UPS-only analysis, the chi-squared test assessing survival direction concordance between our cohort and TCGA-SARC yielded a non-significant result (*p-value*=0.63) (Supplementary Figure 21). This indicates no statistically meaningful agreement in the prognostic impact of gene expression within this subtype across the two datasets.

When extending the analysis to the UPS, DDLPS and LMS samples of the TCGA-SARC, the result remained non-significant (*p-value*= 0.71) (Supplementary Figure 22), suggesting that despite DGE concordance, survival associations do not exhibit consistent directional agreement between cohorts.

To explore the potential causes of this discrepancy, we explored the biological relevance and roles of genes whose expression was significantly associated with a superior OS in the UPS population of the TCGA-SARC cohort. Notably, we observed an association between a substantial enrichment in different immune-related pathways and the expression of genes whose elevated expression levels are correlated with improved prognosis within this universe of UPS samples (Supplementary Figure 23). By contrast, no such enrichment is observed in our study cohort (Supplementary Figure 24), despite the coverage of the same immune-related pathways by the F1RNA gene set (Supplementary Figure 25). This observation suggests that the improved prognosis of

this specific UPS population of the TCGA-SARC cohort may be driven by a distinctive immune enrichment (with a higher preponderance of B cell and humoral-dependent immunoreactivity), which is not verified in our cohort. Consequently, the overall prognostic landscape of the UPS population in TCGA-SARC is biased by the presence of this immunologically distinct subset, limiting the reliability of TCGA-SARC as a validation dataset for survival associations derived from independent studies.

A specific and directed analysis of the molecular data of both the study and the independent cohorts, may clarify the reasons behind this differential immune enrichment (higher B cell and humoral-dependent immunoreactivity) of the UPS population of the TCGA-SARC cohort. Prior studies [51] have demonstrated that indels (generally) and that frameshift indels (more specifically) can serve as potent generators of highly immunogenic neoantigens, leading to increased immunogenicity and activation of humoral immune-related transcriptional programs. We compared the number of indels (Supplementary Figure 26) and frameshift indels (Supplementary Figure 27) per patient across different STS histotypes and observed that, in our study cohort, UPS not only do not exhibit either a higher general indel burden, but also do not show a higher specific frameshift indel burden compared to LMS or DDLPS. On the other hand, in the TCGA-SARC cohort, UPS samples display a markedly higher number of indels per patient relatively to the other two STS histotypes (Supplementary Figure 28). When frameshift indels are specifically analyzed within the TCGA-SARC cohort, no significant differences are found between UPS, LMS and DDLPS (even though, numerically, UPS display a higher number of frameshift indels when compared with LMS and DDLPS) (Supplementary Figure 29). It is important to note that the F1CDx assay utilizes targeted sequencing, whereas TCGA-SARC relies on whole-exome sequencing (WES). Given the differences in sequencing strategies, the absolute number and distribution of indels detected are not directly comparable between cohorts. Therefore, while comparing indel frequencies across subtypes within each cohort is valid, direct comparisons of overall indel burden between the cohorts are not methodologically appropriate.

In summary, immunologically distinct features, likely driven by higher indel loads, appear to influence survival patterns in the TCGA-SARC UPS cohort, limiting its utility for validating prognostic gene expression signatures identified in independent datasets.

SDHB protein is over expressed in UPS and LMS relative to DDLPS

An evaluation of the pattern of expression of the SDHB protein (whose selection was based on the fact that *SDHB* was the only metabolism-related gene whose differential expression in UPS relatively to high-grade LMS and to DDLPS was validated in an independent cohort and whose differential expression was correlated with clinical endpoints in the UPS population of the study cohort) by immunohistochemistry (IHC) was carried out using the same 102 FFPE tumor samples (obtained from a cohort of 101 patients). The clinical and pathological characteristics of this cohort have been thoroughly described in a previous study [42].

IHC for SDHB is typically employed to detect SDH-deficiency, which may manifest either as complete loss of staining in tumor cells or as a range of aberrant cytoplasmic staining patterns [52], in other neoplastic conditions like gastrointestinal stromal tumors, paragangliomas and renal cell carcinomas.

Using IHC to detect differences in SDH granular intensity staining and in intracellular distribution of granules, related with the over expression of SDH subunit encoding genes, is a new challenge that has not been addressed in previous studies.

Although all normal tissues are expected to retain SDH immunoexpression, well established criteria for the quantification of the granular intensity of staining or of the granularity pattern are not established. Therefore, we still rely on a qualitative interpretation of the immunomarker. Accounting for this, we proposed a three-tier score for SDH immunostaining intensity to subdivide and classify variation in retained expression of SDH in sarcoma cases (Figure 4).

When evaluating immunostaining intensity there are important parameters that might influence our interpretation, such as pre-analytic conditions to which specimens were submitted prior to the IHC technique. Moreover, intra-tumoral heterogeneity and cell morphological patterns may influence our evaluation of granular staining intensity, potentially without any direct correlation to underlying genomic and/or transcriptomic alterations.

Sarcomas in general, and especially high-grade / undifferentiated sarcomas, may show areas with different morphologies mixing epithelioid, rhabdoid, pleomorphic and spindle cells. SDH granules are in the cytoplasm. Epithelioid, rhabdoid and pleomorphic cells tend to have a more voluminous cytoplasm and, therefore, effectively more granules that are more easily detectable. Spindle cells, on the other hand, have a scarce and ill-defined cytoplasm, typically showing fewer granularities. Accordingly, staining tends to appear

more intense and diffused in regions rich in epithelioid, rhabdoid and pleomorphic cells, likely reflecting the higher cytoplasmic volume and the associated increase in detectable granules. The opposite occurs for regions rich in spindle cells (Figure 5).

SDHB protein is over expressed in UPS and LMS relatively to DDLPS

DDLPS present the highest absolute and relative number of samples with focal and weak immunostaining (score 1) - 11 samples, corresponding to 42% of all DDLPS samples. Twelve samples (12) showed diffuse and intermediate immunostaining (score 2) (46% of DDLPS samples) and 3 samples evidenced diffuse and strong immunostaining (score 3) (12% of DDLPS samples).

High-grade LMS did not exhibit any sample with focal and weak immunostaining (score 1). The majority of LMS samples presented diffuse and strong immunostaining (score 3) - 16 samples, corresponding to 64% of all LMS samples. The remaining 9 LMS samples (36% of LMS samples) displayed diffuse and intermediate immunostaining (score 2).

UPS show a good balance in terms of the number of samples with diffuse and intermediate immunostaining (score 2) - 26 samples, corresponding to 51% of all UPS samples - and samples with diffuse and strong immunostaining (score 3) - 22 samples, corresponding to 43% of all UPS samples. Only 3 UPS samples (6% of UPS samples) exhibited focal and weak immunostaining (score 1).

Although SDHB expression levels and protein abundance appear higher in UPS and LMS compared to DDLPS, no clear differences can be inferred between UPS and LMS, particularly given the marked undifferentiation, pleomorphism, and intra-tumoral heterogeneity characteristic of UPS. Nonetheless, SDHB overexpression and protein abundance are evident in both UPS and LMS. These findings support the consistent overexpression of SDHB at the protein level in UPS and LMS, reinforcing its potential role as a shared molecular feature of these aggressive STS subtypes.

Metabolomics of UPS, LMS and LPS reveal differences in the metabolome among sarcoma subtypes

Characterization of the patients whose fresh tissue samples were analyzed

An exploratory metabolomic analysis using ^{1}H NMR was conducted on fresh tumor tissue samples from patients with UPS (n=3), LMS (n=3), and LPS (n=2) to further understand the metabolic profile of these STS subtypes. Detailed demographic, pathological, surgical and systemic treatment specificities for the whole cohort of 16 patients from

whom normal and tumor tissue samples were collected are provided in Supplementary Table 7 and Supplementary Table 8.

Metabolomics of UPS, LMS and LPS reveal differences in the metabolome among sarcoma subtypes

A total of 40 metabolites were identified, and their relative levels were compared across samples. While the small sample size limits statistical power and generalizability, 10 metabolites showed significant differences, between at least 2 of the 3 STS subtypes (Figure 6a).

UPS samples exhibited significantly higher levels of branched-chain amino acids (leucine, isoleucine, and valine), phenylalanine, proline, carnosine and uracil relative to LMS, with a similar trend similar trend observed for LPS versus LMS. In contrast, LMS showed higher levels of myo-inositol, NAD^+, and adenine nucleotides (AXP) compared to both UPS and LPS.

These findings highlight distinct metabolic adaptations among STS, which may reflect their contrasts in differentiation status, proliferative capacity, and response to cellular stress.

Succinate levels were significantly lower in LMS compared to LPS when analyzed pairwise. However, no statistically significant differences were observed when comparing all three STS subtypes simultaneously. Fumarate quantification was limited in two samples due to low signal intensity. Notably, the succinate-to-fumarate ratio (n=6) was consistently and significantly higher in UPS compared to both LMS and LPS (Figure 6b), suggesting a potential alteration in SDH-related metabolic activity.

Discussion

The identification of distinctive and specific molecular traits of UPS and the pinpointing of biological differences between UPS, high-grade LMS and DDLPS have been scarcely explored. Isolated single-omics studies, including 10 to 22 UPS and LMS samples, compared the molecular profile of UPS and LMS and highlighted the differential expression of 5 specific miRNAs that target either UPS and LMS-associated genes [53], identified *SRC* differential expression as the best discriminator between UPS and LMS, but failed to discriminate, in a cluster analysis of transcriptomic data, UPS from LMS [54]. To our knowledge, this is the first study that puts the scope on a direct comparative analysis of the molecular profiles of UPS, LMS and DDLPS employing a multi-omics approach.

The gene expression profiling of UPS, high-grade LMS and DDLPS samples included in the study cohort suggests a closer molecular similarity between UPS and high-grade LMS than between UPS and DDLPS, a finding that was posteriorly validated using TCGA-SARC and that is in line with past reports [55].

The over expression of TCA cycle and OXPHOS in UPS results from the relative over expression of *SDHB*, *SDHC* and *SDHD* in this histotype, which was validated, once again, using TCGA-SARC. This validation is particularly relevant considering the fact that the F1RNA gene set was not specifically designed to evaluate the expression profile of metabolism-involved genes, having a low coverage of metabolism-related genes and pathways. Increased mitochondrial activity, broadly, and augmented TCA cycle, specifically, have already been reported for UPS [27,28], although the over expression of *SDH* subunit-encoding genes in UPS is a new finding. SDH functionally couples the flux of the TCA cycle with the electron transport chain (ETC) electron transfer associated with OXPHOS. The SDH mutations, epimutations and specific patterns of expression that are typically found in sarcomas, more commonly in gastrointestinal stromal tumors (GIST), lead to an SDH-deficient phenotype [52,56]. Loss-of-function SDH mutations result in the accumulation of succinate, interfering with dioxygenase function and promoting tumorigenesis [57]. On the other hand, the over expression of *SDH* subunit-encoding genes has been much more scarcely reported than its under expression/silencing in different types of cancer. Nevertheless, the over expression of *SDHA* has been reported in metastatic uveal melanoma [57], advanced ovarian cancer [58] and multiple myeloma [59]. High *SDHA* levels are associated with an elevated OXPHOS respiration capacity, increased expression of proteins that shuttle electrons between different complexes of the ETC and augmented levels of a key TCA enzyme, providing cells with a higher maximal glycolytic capacity, superior total ATP yield, varied bioenergetic profiles and metabolic plasticity, critical tools to meet energetic demands associated with highly proliferative status [57,58]. While *SDHA* encodes a flavoprotein, *SDHB* encodes the iron-sulfur protein that functions as the SDH catalytic core, which is bound to SDHC and SDHD proteins that anchor the whole SDH protein complex, to the inner mitochondrial membrane [58]. Arguably, *SDHB* over expression, like *SDHA* over expression, may equip cells with a similar plethora of bioenergetic tools to sustain highly proliferative status.

The significant correlation between the over expression of *SDHB* and both shorter OS and shorter OS from metastasis date in the specific UPS population of the study cohort should be framed by the notion that the statistical significance of these correlations is

only verified if gene expression is considered a discrete variable. Moreover, while TCGA-SARC shows DGE concordance, it does not show directional agreement in terms of survival associations relatively to the study cohort, not allowing the validation of the associations between the over expression of *SDHB* and clinical endpoints. This may result from the differential survival impact of distinct immunological profiles of the UPS populations of both cohorts, likely driven by the specific higher relative indel load of UPS samples of the TCGA-SARC dataset. The observed over expression of particular immune pathways, such as Antigen Processing and Presentation, is in line with a probably higher humoral and B-cell dependent immunoreactivity of UPS samples of the TCGA-SARC dataset.

The IHC evaluation of the expression of the *SDHB* protein allows the detection of variations in SDH granular intensity staining and in intracellular distribution of SDH granules in relation with the over expression of *SDH* subunit encoding genes. The newly proposed three-tier score for SDH immunostaining intensity permits to classify and subdivide the degrees of expression of SDH in sarcoma cases being, to our knowledge, the first IHC score developed for this purpose. The IHC study reveals that SDHB expression levels and protein abundance are superior in UPS and LMS relatively to DDLPS, in accordance with a crucial part of the findings of the RNA-seq study and adding another layer of validation of one of the main results of the transcriptomic study.

The exploratory characterization of the metabolome using 1^{H} NMR discloses an enrichment in amino acids in UPS samples, possibly reflecting enhanced protein turnover, increased uptake for anabolic growth, or altered transamination activity often associated with aggressive or less differentiated tumors [60]. Uracil levels were also found to be increased in UPS, potentially a result of augmented nucleotide turnover or dysregulated pyrimidine metabolism - hallmarks of enhanced metabolic plasticity and proliferative signaling [61] - supporting the notion that UPS may exhibit higher proliferative capacity than high-grade LMS and DDLPS. The significantly increased levels of carnosine in UPS are noteworthy since this has not been previously described. Carnosine is an endogenous dipeptide with antioxidant and pH-buffering properties, and its higher abundance in UPS may reflect increased oxidative and metabolic stress [62]. Tumor cells combat intracellular acidification by synthesizing carnosine, which helps maintain intracellular pH homeostasis and regulate lysosomal activity. This pH-buffering capacity could also aid in immune evasion, as carnosine modulates the expression of immune-modulatory proteins and protects tumors from T cell-mediated immune surveillance [63]. Altogether, the verified relative increased abundance of carnosine, the

previously reported correlation between the abundance of carnitine and a significantly lower MFS [28], and the previously documented increased TCA cycle activity [27] in UPS all seem to locate critical metabolic adaptations (with correlations with clinical endpoints) in the mitochondria (and possibly at the ETC) of aggressive and progressing UPS. The higher levels of myo-inositol in LMS may be a product of increased membrane turnover or phosphoinositide signaling (tightly involved in calcium homeostasis, contractility and membrane remodeling in smooth muscle cells), besides being consistent with tissue lineage [64]. Finally, higher NAD^+ and AXP levels suggest a more regulated redox state and preserved bioenergetic balance in LMS.

The evaluation of succinate and fumarate levels in the NMR spectra provides valuable insights. Even though no significant differences in succinate levels were found between UPS and both LMS and LPS samples, the higher succinate-to-fumarate ratio in UPS offers precious clues. This elevated succinate-to-fumarate ratio, despite SDHB over expression, can indicate functional impairment of SDH enzymatic activity, possibly due to post-translational modifications, altered assembly of SDH subunits, or imbalanced TCA flux. This metabolic signature may be consistent with prior observations in certain aggressive tumors, where succinate accumulates as an oncometabolite, potentially contributing to pseudohypoxia by inhibiting prolyl hydroxylases and stabilizing HIF-1α, thus promoting tumor progression [65]. Curiously, intracellular succinate accumulation may improve antigen presentation by the transcriptional and epigenetic activation of major histocompatibility complex–antigen processing and presentation genes (MHC-APP) genes, potentially enhancing tumor immunogenicity [66]. Further studies are necessary to clearly identify SDH enzymatic activity patterns in UPS, to highlight relative and absolute succinate levels in UPS and to clarify the relationship between intracellular succinate levels and different immunogenicity profiles among UPS. This is relevant since the UPS diverse immune microenvironmental composition is known to impact prognosis (denser infiltration by CD8+T lymphocytes and monocytes is associated with significantly better MFS and OS [67,68], while, on the other hand, denser infiltration with CD8+T lymphocytes and CD20+B lymphocytes is associated both with good prognosis overall, but also with poor response to neoadjuvant chemotherapy [69]).

There is, indeed, a growing body of evidence that links succinate levels of both tumor cells and microenvironmental CD8+ T cells to different profiles of anti-tumor immunogenicity and to a distinct immune composition of the tumor microenvironment. Succinate is, beyond coupling the flux of the TCA cycle with the ETC electron transfer associated with OXPHOS, a powerful regulator of epigenetic pathways that control

cellular features relevant to cancer and immunotherapy [70]. Succinate mediates transcriptional and epigenetic activation of MHC-APP independent of interferon signaling in melanoma cells, and intracellular succinate accumulation has been shown to improve antigen presentation [66]. It is interesting to note that the employment of therapeutic strategies that redirect the electron flux through specific ETC complexes (shifting electron shuttling away from complex II (SDH)) rewires ETC activity, increases intracellular succinate levels, and achieves antitumor responses without significant side effects [66]. Otherwise, the accumulation of succinate downstream of mitochondrial prolyl 4 hydroxylase subunit alpha 1, as elicited by chronic TCR signaling, in CD8+ T cells has been shown to reinforce T cell exhaustion and limit tumor sensitivity to immunotherapy [65].

This study has several limitations that are crucial to underline. The retrospective nature must be mentioned. The gene expression analysis is cumulated by diverse caveats. The samples pool that was used is comprised by samples of a limited number of STS hitotypes, primary tumor samples of a great majority of STS patients with early stage disease (there is neither a significant representation of samples obtained from STS metastases nor of advanced STS cases), and by samples collected in different timepoints and with heterogenous chronological ages (displaying distinct degrees of biological degradation, impacting the number of samples for which the quality control of RNA-seq was not successful). The sequencing tests that were used are targeted sequencing tests, offering a different coverage than a whole genome or exome sequencing approach. Finally, the F1RNA gene set has, as mentioned, a low coverage of the metabolism-related genes and pathways. The characterization of the metabolome also has particular limitations itself. The size of this samples set is particularly small (even more striking when the scope is put on the number of samples of the specific STS subtypes we intended to study) and its composition per sarcoma subtype is heterogenous. There is a notable dispersion in terms of histological grade, topographical location and tissue of origin of the samples. These two sets were not built with the same biopsy or surgical samples collected from the same patients. There are crucial differences in the histopathological composition (e.g., the pool of FFPE LPS samples corresponded exclusively to DDLPS, while the pool of fresh tissue LPS samples was composed by 1 sample of DDLPS and 1 sample of MLPS), and in the tumor grade (e.g. all STS FFPE samples were grade 3, while 1 LMS fresh tissue sample was grade 2, and 2 LPS fresh tissue samples were grade 2) of each of these samples sets.

This plethora of new findings should be prospectively validated in a larger and more homogenous set of paired fresh tissue and FFPE tumor samples of different high-grade bone and soft tissue sarcomas. This validation should also be performed with a multi-omics analytical design, adding new omics (namely proteomics) to the ones that have been used in the present study. The findings reported here open several possible future lines of research. More preliminary (*in vitro* and *in vivo*) studies are needed to validate the clinical value of interfering with SDH levels and/or function, and with succinate levels. If a link between variations in succinate levels and antigen presentation/processing capacity/nature of immune response is demonstrated, then the exploration of sequential combinations between ETC electron flux modulators and immune checkpoint inhibitors (in different timings) is amply justified. Nevertheless, in our perspective, the agents tested for this purpose should not be restricted to direct inhibitors of SDH subunits, as a predictable associated neurotoxicity of SDH inhibitors could preclude its use, and also because, mechanistically, the biological advantage of UPS cells may not be linearly associated with increased enzymatic activity directly associated with SDHB increased expression, but might be based on functional impairment of SDH enzymatic activity, which may lead to intracellular accumulation of succinate.

References

[1] Gronchi, A., Miah, A.B., Dei Tos, A.P., et al. Soft tissue and visceral sarcomas: ESMO-EURACAN-GENTURIS Clinical Practice Guidelines for diagnosis, treatment and follow-up. *Ann. Oncol*. 32 (11), 1348-1365 (2021).

[2] Connolly, E.A., Grimison, P.S., Horvath, L.G., et al. Quantitative proteomic studies addressing unmet clinical needs in sarcoma. *Front Oncol*. 13,1126736 (2023).

[3] American Cancer Society. *Cancer Facts & Figures 2025*. Atlanta: American Cancer Society; 2025. Available at https://www.cancer.org/research/cancer-facts-statistics/all-cancer-facts-figures/2025-cancer-facts-figures.html.

[4] Toro, J.R., Travis, L.B., Wu, H.J., et al. Incidence patterns of soft tissue sarcomas, regardless of primary site, in the surveillance, epidemiology and end results program, 1978–2001: An analysis of 26,758 cases. *Int J Cancer*. 2006; 119: 2922–2930.

[5] Vodanovich, D.A., Spelman, T., May, D., et al. Predicting the prognosis of undifferentiated pleomorphic soft tissue sarcoma: a 20-year experience of 266 cases. *ANZ J Surg*. 2019; 89(9):1045-1050.

[6] Winchester, D., Lehman, J., Tello, T., et al. Undifferentiated pleomorphic sarcoma: Factors predictive of adverse outcomes. *J Am Acad Dermatol*. 2018;79(5):853-859.

[7] Goldblum, J.R. An approach to pleomorphic sarcomas: can we subclassify, and does it matter? *Mod Pathol*. 2014; 27 (1): 39-46.

[8] Ozzello, L., Stout, A.P., Murray, M.R. Cultural characteristics of malignant histiocytomas and fibrous xanthomas. *Cancer*. 1963;16:331–344.

[9] O'Brien, J.E., Stout, A.P. Malignant fibrous xanthomas. *Cancer*. 1964;17:1445–1455.

[10] Iwasaki, H., Isayama, T., Johzaki, H., et al. Malignant fibrous histiocytoma. Evidence of perivascular mesenchymal cell origin immunocytochemical studies with monoclonal anti-MFH antibodies. *Am. J. Pathol*. 1987;128:528–537.

[11] Iwasaki, H., Isayama, T., Ohjimi, Y., et al. Malignant fibrous histiocytoma. A tumor of facultative histiocytes showing mesenchymal differentiation in cultured cell lines. *Cancer*. 1992; 69:437–447.

[12] Roholl, P.J., Kleyne, J., Elbers, H., et al. Characterization of tumour cells in malignant fibrous histiocytomas and other soft tissue tumours in comparison with malignant histiocytes. I. Immunohistochemical study on paraffin sections. *J Pathol*. 1985;147:87–95.

[13] Roholl, P.J., Kleyne, J., Van Unnik, J.A. Characterization of tumor cells in malignant fibrous histiocytomas and other soft-tissue tumors, in comparison with malignant

histiocytes. II. Immunoperoxidase study on cryostat sections. *Am J Pathol*. 1985;121:269–274.

[14] Montgomery, E., Fisher, C. Myofibroblastic differentiation in malignant fibrous histiocytoma (pleomorphic myofibrosarcoma): a clinicopathological study. *Histopathology*. 2001;38:499–509.

[15] Massi, D., Beltrami, G., Capanna, R., et al. Histopathological re-classification of extremity pleomorphic soft tissue sarcoma has clinical relevance. *Eur J Surg Oncol*. 2004;30:1131–1136.

[16] Guled, M., Pazzaglia, L., Borze, I., et al. Differentiating Soft Tissue Leiomyosarcoma and Undifferentiated Pleomorphic Sarcoma: A miRNA Analysis. *Genes Chromosomes Cancer*. 2014; 53 (8): 693-702.

[17] Villacis, R.A.R, Silveira, S.M., Barros-Filho, M.C., et al. Gene Expression Profiling in Leiomyosarcomas and Undifferentiated Pleomorphic Sarcomas: SRC as a New Diagnostic Marker. *PLoS ONE*. 2014; 9(7): e102281.

[18] Deyrup, A.T., Haydon, R.C., Huo, D., et al. Myoid differentiation and prognosis in adult pleomorphic sarcomas of the extremity: an analysis of 92 cases. *Cancer*. 2003;98:805–813.

[19] Fletcher, C.D., Gustafson, P., Rydholm, A., et al. Clinicopathologic re-evaluation of 100 malignant fibrous histiocytomas: prognostic relevance of subclassification. *J Clin Oncol*. 2001;19:3045–3050.

[20] Zou, Z., Sun, W., Xu, Y., et al. Application of Multi-Omics Approach in Sarcomas: A Tool for Studying Mechanism, Biomarkers, and Therapeutic Targets. *Front. Oncol*. 2022, 12, 946022.

[21] Hollywood, K., Brison, D.R., Goodacre, R. Metabolomics: Current technologies and future trends. *Proteomics.* 2006, 6, 4716–4723.

[22] Rinschen, M.M., Ivanisevic, J., Giera, M., et al. Identification of bioactive metabolites using activity metabolomics. *Nat. Rev. Mol. Cell Biol*. 2019, 20, 353–367.

[23] Han, J., Li, Q., Chen, Y., et al. Recent Metabolomics Analysis in Tumor Metabolism Reprogramming. *Front. Mol. Biosci*. 2021, 8, 763902.

[24] Baker, S.A., Rutter, J. Metabolites as signaling molecules. *Nat. Rev. Mol. Cell Biol*. 2023, 24, 355-374.

[25] Miallot, R., Galland, F., Millet, V., et al. Metabolic landscapes in sarcomas. *J. Hematol. Oncol*. 2021, 14, 114.

[26] Kelly, A.D.; Breitkopf, S.B.; Yuan, M.; Goldsmith, J.; Spentzos, D.; Asara, J.M. Metabolomic Profiling from Formalin-Fixed, Paraffin-Embedded Tumor Tissue Using Targeted LC/MS/MS: Application in Sarcoma. PLoS ONE 2011, 6, e25357.
[27] Lee, P.; Malik, D.; Perkons, N.; Huangyang, P.; Khare, S.; Rhoades, S.; Gong, Y.-Y.; Burrows, M.; Finan, J.M.; Nissim, I.; et al. Targeting glutamine metabolism slows soft tissue sarcoma growth. Nat. Commun. 2020, 11, 498.
[28] Lou, S.; Balluff, B.; Cleven, A.H.G.; Bovée, J.V.M.G.; McDonnell, L.A. Prognostic Metabolite Biomarkers for Soft Tissue Sarcomas Discovered by Mass Spectrometry Imaging. J. Am. Soc. Mass Spectrom. 2017, 28, 376–383.
[29] Negendank,W.G. MR Spectroscopy of musculoskeletal soft tissue tumors. Magn. Reson. Imaging Clin. N. Am. 1995, 3, 713–725.
[30] Li, C.W.; Kuesel, A.C.; Padavic-Shaller, K.A.; Murphy-Boesch, J.; Eisenberg, B.L.; Schmidt, R.G.; von Roemeling, R.W.; Patchefsky, A.S.; Brown, T.R.; Negendank, W.G. Metabolic characterization of human soft tissue sarcomas in vitro and in vivo using proton decoupled phosphorous magnetic resonance spectroscopy. Cancer Res. 1996, 56, 2964–2972.
[31] Jayashree, B.; Deshmukh, S.; Rajkumar, T. Assessment of human sarcoma tissues by proton NMR spectroscopy: Correlation with histopathology. Curr. Sci. 1999, 77, 587–592.
[32] Singer, S.; Millis, K.; Souza, K.; Fletcher, C. Correlation of lipid content and composition with liposarcoma histology and grade. Ann. Surg. Oncol. 1997, 4, 557–563.
[33] Singer, S.; Sivaraja, M.; Souza, K.; Millis, K.; Corson, J.M. H-NMR detectable fatty acyl chain unsaturation in excised leiomyosarcoma correlate with grade and mitotic activity. J. Clin. Investig. 1996, 98, 244–250.
[34] Millis, K.K.; Mass, W.E.; Cory, D.G.; Singer, S. Gradient, high-resolution, magic-angle spinning nuclear magnetic resonance spectroscopy of human adipocyte tissue. Magn. Reson. Med. 1997, 38, 399–403.
[35] Millis, K.;Weybright, P.; Campbell, N.; Fletcher, J.A.; Fletcher, C.D.; Cory, D.G.; Singer, S. Classification of human liposarcoma and lipoma using ex vivo proton NMR spectroscopy. Magn. Reson. Med. 1999, 41, 257–267.
[36] Bezabeh, T.; El-Sayed, S.; Patel, R.; Somorjai, R.L.; Bramwell, V.; Kandel, R.; Smith, I.C.P. Statistical classification strategy for proton magnetic resonance spectra of soft tissue sarcoma: An exploratory study with potential clinical utility. Sarcoma 2002, 6, 97–103.

[37] Wang, C.-K.; Li, C.-W.; Hsieh, T.-J.; Chien, S.-H.; Liu, G.-C.; Tsai, K.-B. Characterization of bone and soft-tissue tumors with in vivo 1H MR Spectroscopy: Initial Results. Radiology 2004, 232, 599–605.

[38] Sharma, U.; Kar, M.; Juyal, S.; Deo, S.; Jagannathan, N.R. Biochemistry of Soft Tissue Tumors: As In Vitro NMR Study. Proc. Int. Soc. Magn. Reson. Med. 2007, 15, 3682.

[39] Di Gialleonardo, V.; Aldeborgh, H.N.; Miloushev, V.; Folkers, K.M.; Granlund, K.; Tap,W.D.; Lewis, J.S.;Weber,W.A.; Keshari, K.R. Multinuclear NMR and MRI reveal an early metabolic response to mTOR inhibition in sarcoma. Cancer Res. 2017, 77, 3113–3120.

[40] Mercier, K.A.; Al-Jazrawe, M.; Poon, R.; Acuff, Z.; Alman, B. A metabolomics pilot study on desmoid tumors and novel drug candidates. Sci. Rep. 2018, 8, 584.

[41] Masiewicz, E.; Ashcroft, G.P.; Boddie, D.; Dundas, S.R.; Kruk, D.; Broche, L.M. Towards applying NMR relaxometry as a diagnostic tool for bone and soft tissue sarcomas: A pilot study. Sci. Rep. 2020, 10, 14207.

[42] Esperança-Martins, M., Vasques, H., Sokolov Ravasqueira, M., et al. Machine learning-based analysis of genomic and transcriptomic data unveils sarcoma clusters with superlative prognostic and predictive value. medRxiv 2025.01.31.25321492; doi:https://doi.org/10.1101/2025.01.31.25321492.

[43] Milbury, C.A., Creeden, J., Yip, W-K, et al. Clinical and analytical validation of FoundationOne®CDx, a comprehensive genomic profiling assay for solid tumors. PLoS One. 17(3), e0264138 (2022).

[44] Sun, D., Huang, R.S.P., Green, M., et al. Analytical Validation of FoundationOne RNA Assay For Fusion Detection In 189 Clinical Tumor Specimens. Poster presented at AMP 2023; November, 14-18, 2023.

[45] Chen, Y., Chen, L., Lun, A.T.L, et al. edgeR 4.0: powerful differential analysis of sequencing data with expanded functionality and improved support for small counts and larger datasets. bioRxiv. doi:10.1101/2024.01.21.576131 (2024).

[46] Ritchie, M.E., Phipson, B., Wu, D., Hu, Y., Law, C.W., Shi, W., Smyth, G.K. limma powers differential expression analyses for RNA-sequencing and microarray studies. Nucleic Acids Res. 43(7), e47 (2015).

[47] Kanehisa, M., Furumichi, M., Sato, Y., Matsuura, Y. and Ishiguro-Watanabe, M.; KEGG: biological systems database as a model of the real world. Nucleic Acids Res. 53, D672-D677 (2025).

[48] Therneau, T.M., Grambsch, P.M. Modeling Survival Data: Extending the Cox Model. Springer, New York. ISBN 0-387-98784-3 (2000).
[49] Xu S, Hu E, Cai Y, Xie Z, Luo X, Zhan L, Tang W, Wang Q, Liu B, Wang R, Xie W, Wu T, Xie L, Yu G (2024). “Using clusterProfiler to characterize multiomics data.” Nature Protocols, 19(11), 3292-3320.
[50] Cancer Genome Atlas Research Network. Comprehensive and integrated genomic characterization of adult soft tissue sarcomas. *Cell*. 171(4), 950–965 (2017).
[51] Turajlic, S., Litchfield, K., Xu, H., Rosenthal, R., McGranahan, N., Reading, J. L., ... & Swanton, C. (2017). Insertion-and-deletion-derived tumour-specific neoantigens and the immunogenic phenotype: a pan-cancer analysis. The lancet oncology, 18(8), 1009-1021.
[52] Ding, C-K., Chan, S., Mak, J., et al. An exploration in pitfalls in interpreting SDHB immunohistochemistry. Histopathology. 81 (2), 264-269. (2022)
[53] Guled, M., Pazzaglia, L., Borze, I., et al. Differentiating Soft Tissue Leiomyosarcoma and Undifferentiated Pleomorphic Sarcoma: A miRNA Analysis. *Genes Chromosomes Cancer*. 2014; 53 (8): 693-702.
[54] Villacis, R.A.R, Silveira, S.M., Barros-Filho, M.C., et al. Gene Expression Profiling in Leiomyosarcomas and Undifferentiated Pleomorphic Sarcomas: SRC as a New Diagnostic Marker. *PLoS ONE*. 2014; 9(7): e102281.
[55] Carneiro, A., Francis, P., Bendahl, P-O., et al. Indistinguishable genomic profiles and shared prognostic markers in undifferentiated pleomorphic sarcoma and leiomyosarcoma: different sides of a single coin?. Lab Invest. 2009; 89(6): 668-675.
[56] Cervera, A., Apostolova, N., Crespo, F.L., et al. Cells Silenced for SDHB Expression Display Characteristic Features of the Tumor Phenotype. Cancer Res. 2008; 68 (11): 4058-4067.
[57] Chattopadhay, C., Oba, J., Roszik, J., et al. Elevated Endogenous SDHA Drives Pathological Metabolism in Highly Metastatic Uveal Melanoma. *Invest. Ophthalmol. Vis. Sci.* 2019; 60(13): 4187-4195.
[58] Wang, L., Cybula, M., Rostworowska, M., et al. Upregulation of Succinate Dehydrogenase (SDHA) Contributes to Enhanced Bioenergetics of Ovarian Cancer Cells and Higher Sensitivity to Anti-Metabolic Agent Shikonin. Cancers. 2022; 14: 5097.
[59] Sun, Y., Xu, Z., Jiang, J., et al. High Expression of Succinate Dehydrogenase Subunit A Which Is Regulated by Histone Acetylation, Acts as a Good Prognostic Factor of Multiple Myeloma Patients. Front Oncol. 2020;10:563666.

[60] Liu, X., Ren, B., Ren, J. et al. The significant role of amino acid metabolic reprogramming in cancer. Cell Commun Signal. 2024; 22: 380.

[61] Mullen, N.J., Singh, P.K. Nucleotide metabolism: a pan-cancer metabolic dependency. Nat Rev Cancer. 2023; 23(5):275-294.

[62] Boldyrev AA, Aldini G, Derave W. Physiological and pathophysiological roles of carnosine. Biochim Biophys Acta. 2013;1832(6):1132–1141.

[63] Carnosine helps cancer cells to evade immune surveillance by regulating intracellular pH. Nat Immunol. 2024; 25: 399–400.

[64] Di Paolo, G., De Camilli, P. Phosphoinositides in cell regulation and membrane dynamics. Nature 443, 651–657 (2006). https://doi.org/10.1038/nature05185.

[65] Selak, M.A., Armour, S.M., MacKenzie, E.D., et al. Succinate links TCA cycle dysfunction to oncogenesis by inhibiting HIF-alpha prolyl hydroxylase. Cancer Cell. 2005; 7(1): 77-85.

[66] Mangalhara, K.C., Varanasi, S.K., Johnson, M.A., et al. Manipulating mitochondrial electron flow enhances tumor immunogenicity. Science. 2023; 381(6664): 1316-1323.

[67] Toulmonde, M., Lucchesi, C., Verbeke, S., et al. High throughput profiling of undifferentiated pleomorphic sarcomas identifies two main subgroups with distinct immune profile, clinical outcome and sensitivity to targeted therapies. EBioMedicine. 2020; 62: 103131.

[68] Lazcano, R., Barreto, C.M., Salazar, R., et al. The immune landscape of undifferentiated pleomorphic sarcoma. Front. Oncol. 2022; 12:1008484.

[69] Guegan, J.P., El Ghazzi, N., Vibert, J., et al. Predictive value of tumor microenvironment on pathologic response to neoadjuvant chemotherapy in patients with undifferentiated pleomorphic sarcomas. Journal of Hematology & Oncology. 2024; 17: 100.

[70] Galluzi, L., Guilbaud, E., and Garg, A.D. Mitochondrial succinate feeds T cell exhaustion in cancer. Cancer Cell. 2025; 43 (2): 168-170.

Declarations

Ethics Approval and Consent to Participate

The present study was performed in accordance with the ethical standards of Helsinki Declaration II and was approved by the Institution Review Boards of both CAML and IPOLFG.

Consent for Publication

Not Applicable.

Competing Interests

Miguel Esperança-Martins (MEM)

Research Grants: Hoffmann-LaRoche, Foundation Medicine Inc., PharmaMar;

Invited Speaker: Bayer;

Advisory Boards: Gilead.

Richard S.P. Huang (RH)

Richard Huang is an employee of Foundation Medicine Inc, a wholly owned subsidiary of Roche and receives stocks from Roche

Isabel Fernandes (IF)

Research Grants: MSD; PharmaMar.

Brian Van Tine (BVT)

Brian A. Van Tine reports research grants from Polaris Pharmaceuticals and personal fees from consulting from Aadi Bioscience, Actua Capital Partners LLC, Advenchen Laboratories, Boxer Capital LLC, Crisper Therapeutics, Deciphera Pharmaceuticals Inc., Daiichi Sankyo Company, EcoR1 Capital LLC, Galapagos, Hinge Bio, Putnam, Sonata Therapeutics, and Salarius Pharmaceuticals Inc.; Honoraria for educational talks from Beijing Biostar Pharmaceuticals, Co., LTD., Oncology Education, and Total Health Conference; participation on a data/safety advisory board for Daiichi Sankyo, Bayer US Medical Affairs, PTC Therapeutics, Aadi Biosciences, Boehringer Ingelheim, Regeneron Pharmaceuticals, Curis, Syneos Health, Deciphera Pharmaceuticals, and Curtis; nonpaid service as a board member with Polaris; travel support from Adaptimmune LLC; licensing/patents with Accuronix Therapeutics.

Luis Costa (LC)

Research Grants: MSD; Eli Lilly; Amgen, Roche, Janssen;

Invited Speaker: Hoffmann-LaRoche, Gilead; AstraZeneca; Eli Lilly; MSD; BMS, Astellas.

Advisory Boards: Roche; AstraZeneca; Bayer; Pfizer; Gilead, Novartis; Servier.

Funding

DNA and RNA sequencing tests (FoundationOne®CDx and FoundationOne®RNA) and DNA and RNA sequencing performance were sponsored by F.Hoffmann-LaRoche AG and by Foundation Medicine Inc under the RNA LDT Research Programme.

Different laboratory reagents and materials employed for the immunohistochemistry and ^{1}H NMR assays were sponsored by PharmaMar.

Authors' Contributions

Authors Initials

Miguel Esperança-Martins (MEM) (First and Corresponding Author)

Hugo Vasques (HV)

Manuel Sokolov Ravasqueira (MSR)

Filipa Santos (FS)

Filipa Fonseca (FF)

António Syder Queiroz (ASQ)

João Boavida (JB)

Daniel Martins Jordão (DMJ)

Joaquim Soares do Brito (JSB)

Patrícia Corredeira (PC)

Marta Martins (MM)

Ângela Afonso (AA)

Jorge Antonio López (JAL)

Richard S.P.Huang (RH)

Cecília Melo-Alvim (CMA)

Isabel Fernandes (IF)

Dolores López-Presa (DLP)

Maria Manuel Lemos (MML)

Brian Van Tine (BVT)

Alliny Bastos (AB)

Sandra Casimiro (SC)

Nuno Abecasis (NA)

Luís Costa (LC)

Emanuel Gonçalves (EG)

Iola Duarte (ID)

Sérgio Dias (SD)

Contributions

Contribution of each of the authors

Conceptualization: MEM, HV, MSR, FS, IF, MML, BVT, AB, LC, EG, ID, SD.

Methodology: MEM, HV, MSR, FS, MML, SC, EG, ID, SD.

Investigation: MEM, HV, MSR, FS, FF, ASQ, JB, DMJ, JSB, PC, MM, AA, CMA, DLP, MML, SC, EG, ID, SD.

Visualization: MEM, MSR, FS, FF, PC, MML, SC, EG, ID, SD.

Funding acquisition: MEM, HV, IF.

Project administration: MEM, HV, IF, SD.

Supervision: HV, JAL, RH, IF, MML, BVT, AB, SC, NA, LC, EG, ID, SD.

Writing – original draft: MEM, HV, MSR, FS, FF, ASQ, MML, SC, EG, ID, SD.

Writing – review & editing: MEM, MSR.

Acknowledgements

This research was sponsored by F.Hoffmann-LaRoche AG and by Foundation Medicine Inc under the RNA LDT Research Programme and also by PharmaMar. We would like to thank F.Hoffmann-LaRoche AG and Foundation Medicine Inc for providing the FoundationOne®CDx and FoundationOne®RNA assays, and for all the technical support, specifically during the transfer of the sequencing data via the safe platform. We would also like to thank PharmaMar for sponsoring the acquisition of laboratory reagents and materials.

We would like to thank Sarah Yacoub (Foundation Medicine Inc) for all the precious help in the logistical operationalization of the transfer of all of the different batches of samples between iMM (Lisbon, Lisbon, Portugal) and the Foundation Medicine Headquarters (Cambridge, Massachusetts, United States of America) and for her valuable assistance on sending the results of both DNA and RNAseq results via a safe platform.

We would also like to thank Rachel Beth Keller-Evans (Foundation Medicine Inc) for her crucial support in the analysis of the data that has resulted from the employment of the FoundationOne®RNA assay, namely for her help in the analysis of the detected fusions. We would also like to show our deepest gratitude to the IPOLFG tumor biobank staff (that were responsible for the original retrieval and organization both of the FFPE samples and also of some of the fresh tissue samples that were used in this study), the IPOLFG pathology department staff (who developed, in collaboration with the IPOLFG pathologists, the protocol for SDHB immunostaining, who assisted both the two pathologists that scored SDHB immunoreactivity and also the pathologist that reviewed each FFPE sample), the iMM biobank staff (that were responsible for the collection, storage and organization of the majority of the fresh tissue samples that were used in this study, and that were also responsible for the preparation and shipment of fresh tissue samples to CICECO (Aveiro, Portugal) for the ^{1}H NMR evaluation), the iMM Comparative Pathology unit team (that have sectioned the FFPE blocks), the iMM Translational Oncobiology Lab staff (that have helped in the preparation and shipment of the different batches of samples and that have also played a key role in the development of the protocol for SDHB immunostaining), the iMM Technology Transfer Office staff, and the CICECO staff (who have played a crucial role in the logistical operationalization of the ^{1}H NMR evaluation).

Figure Legends

Figure 1 *- Limma-Voom differential expression of SDHA, SDHB, SDHC and SDHD for comparative evaluations between UPS, high-grade LMS, and DDLPS. For each SDH differential gene expression analysis (between different high-grade STS subtypes) adjusted p-values and logFC values are provided.*

Figure 2 *- Correlations, within the UPS population, between the over expression of SDHB and OS, either using the KMM (**Figure 2a**) and also using a CHPM (**Figure 2b**), and between the over expression of SDHB and OS from metastasis date, either using the KMM (**Figure 2c**) and also using a CPHM (**Figure 2d**).*

Figure 3 *- Limma-Voom differential expression of SDHA, SDHB, SDHC and SDHD for comparative evaluations between UPS, high-grade LMS, and DDLPS samples of an independent cohort (TCGA-SARC). For each SDH differential gene expression analysis (between different high-grade STS subtypes) adjusted p-values and logFC values are provided.*

Figure 4 *- SDHB immunohistochemistry in sarcomas: Three-tier score for SDH immunostaining intensity - A and B with weak and focal granular cytoplasmic immunostaining (score 1); C and D with diffuse intermediate granular cytoplasmic immunostaining (score 2); E and F with diffuse and strong granular cytoplasmic immunostaining (score 3).*

Figure 5 *- SDHB immunohistochemistry in sarcomas: Differences in immunostaining intensity related to tumoral heterogeneity and cell morphology - Spindle cells with scarce and ill-defined cytoplasm tend to show a more focal and weak staining (A); epithelioid and pleomorphic cells, as well as multinucleated giant cells, with a more voluminous cytoplasm tend to show more granularity and diffusely intense staining (B and C).*

Figure 6

Figure 6a) *- Metabolites whose abundance was significantly different between at least two of the three STS subtypes.*

Figure 6b) *- Succinate levels and succinate-to-fumarate ratio across STS subtypes.*

Figure 1

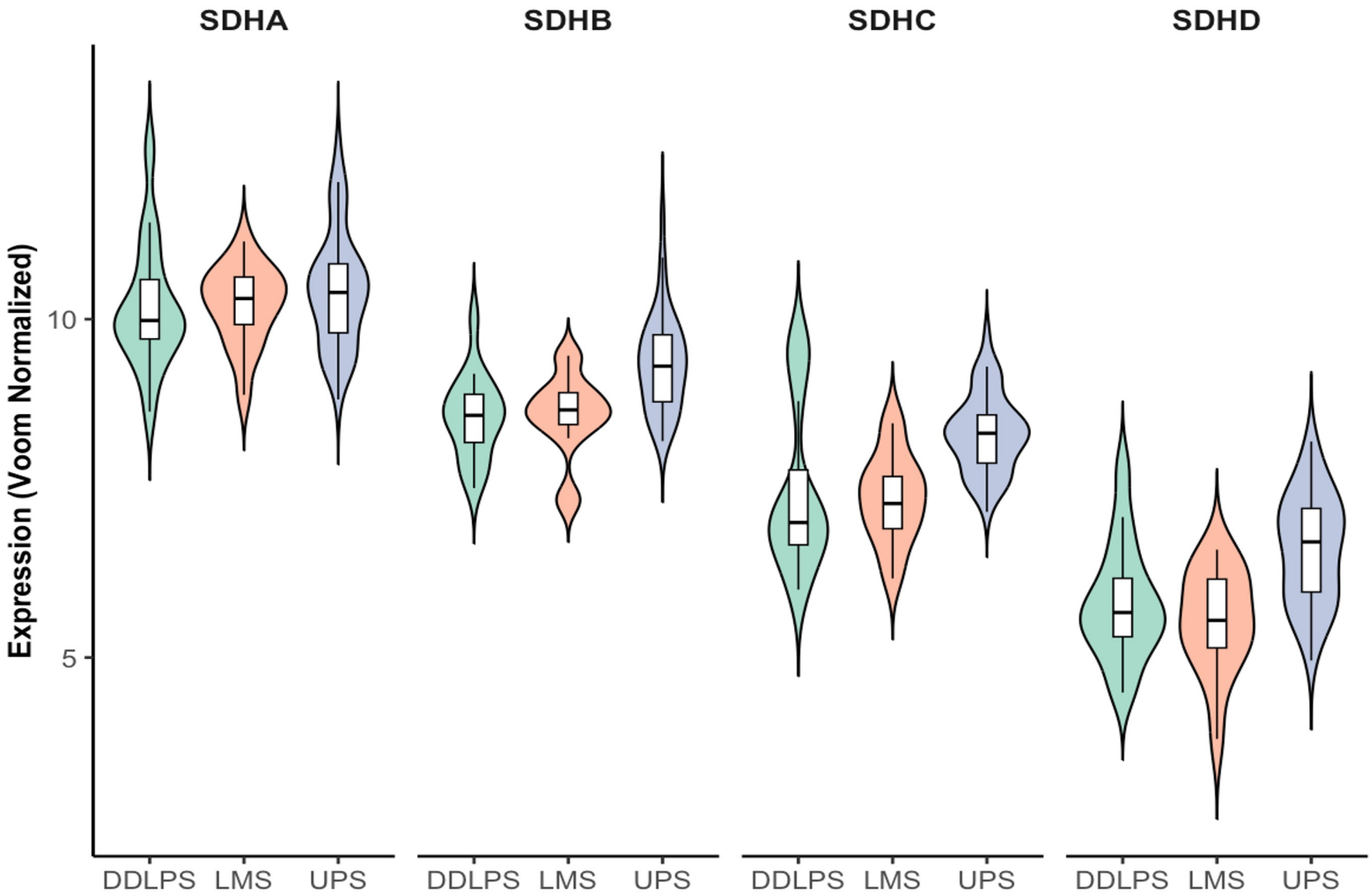

SDHA Differential Gene Expression

Comparison	adj_p_value	logfc
LMS VS DDLPS	0.979	0.025
UPS vs LMS	0.658	0.22
UPS vs DDLPS	0.523	0.246

Note. Limma-Voom Differential expression results

SDHB Differential Gene Expression

Comparison	adj_p_value	logfc
LMS VS DDLPS	0.963	0.033
UPS vs LMS	0.019	0.764
UPS vs DDLPS	0.002	0.797

Note. Limma-Voom Differential expression results

SDHC Differential Gene Expression

Comparison	adj_p_value	logfc
LMS VS DDLPS	0.904	-0.086
UPS vs LMS	0.013	0.965
UPS vs DDLPS	0.003	0.879

Note. Limma-Voom Differential expression results

SDHD Differential Gene Expression

Comparison	adj_p_value	logfc
LMS VS DDLPS	0.729	-0.228
UPS vs LMS	0.013	1.059
UPS vs DDLPS	0.009	0.831

Note. Limma-Voom Differential expression results

Figure 2

Figure 2a)

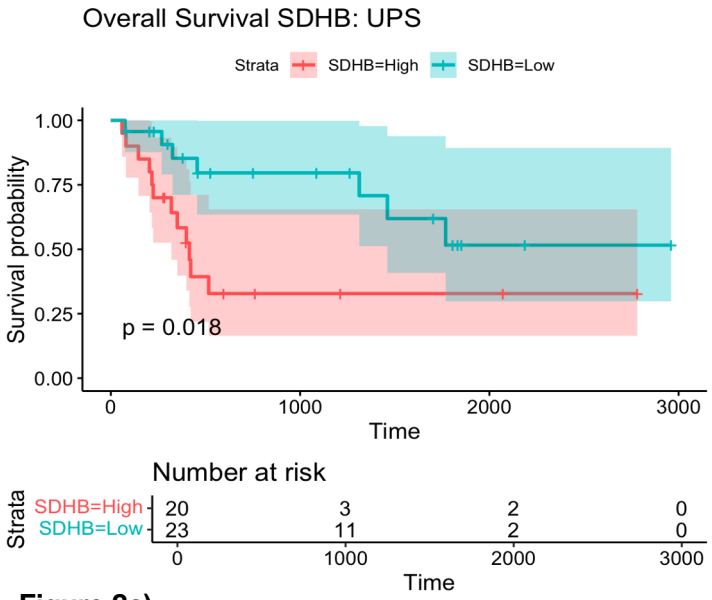

Figure 2b)

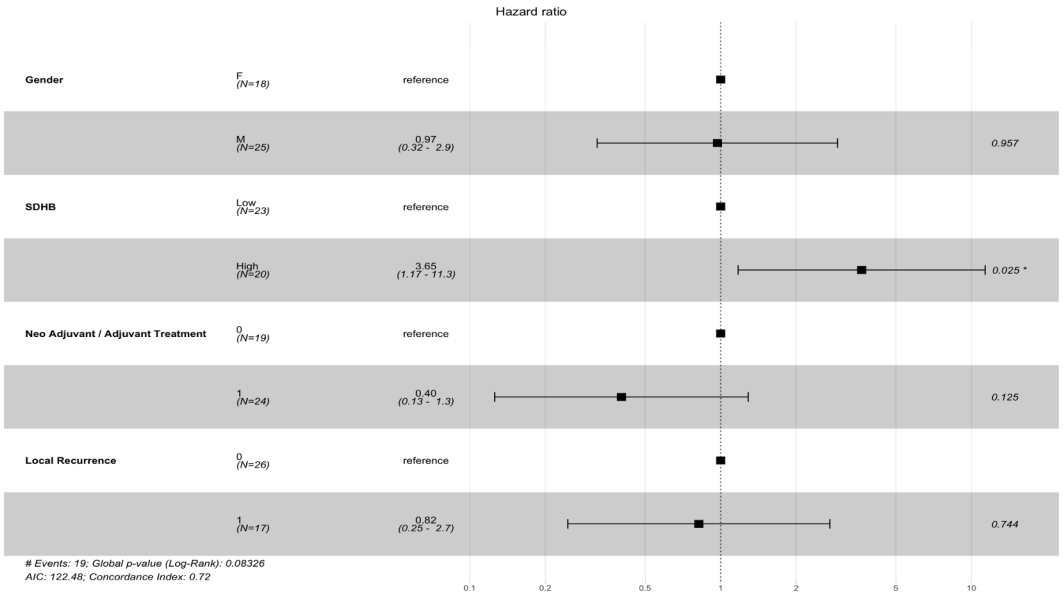

Figure 2c)

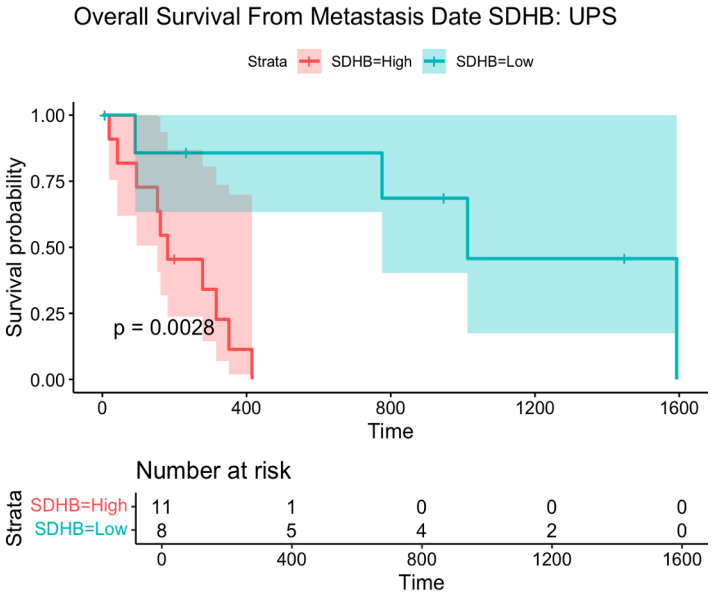

Figure 2d)

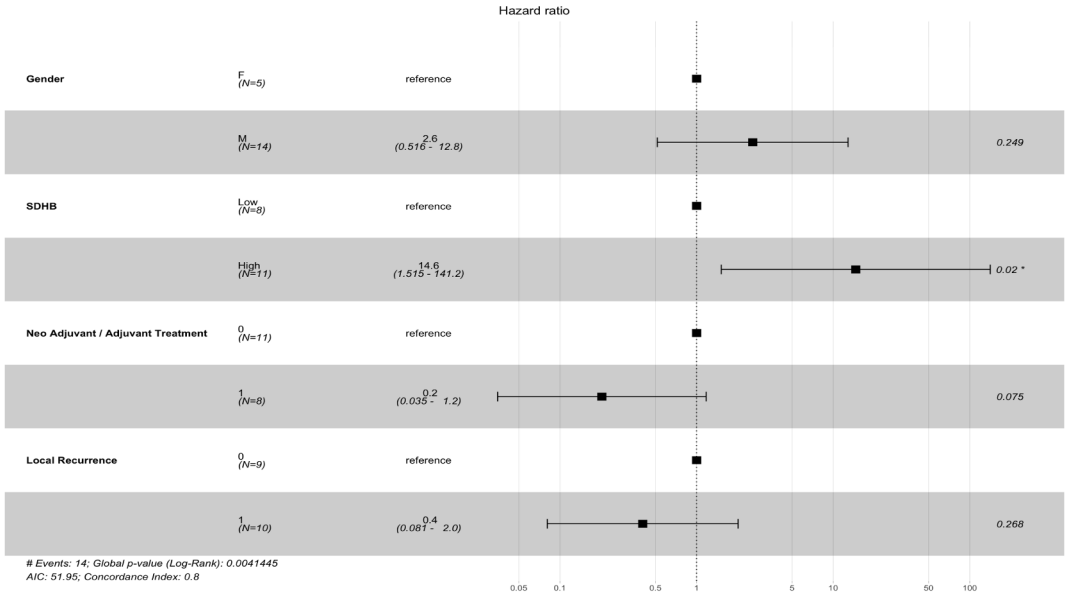

Figure 3

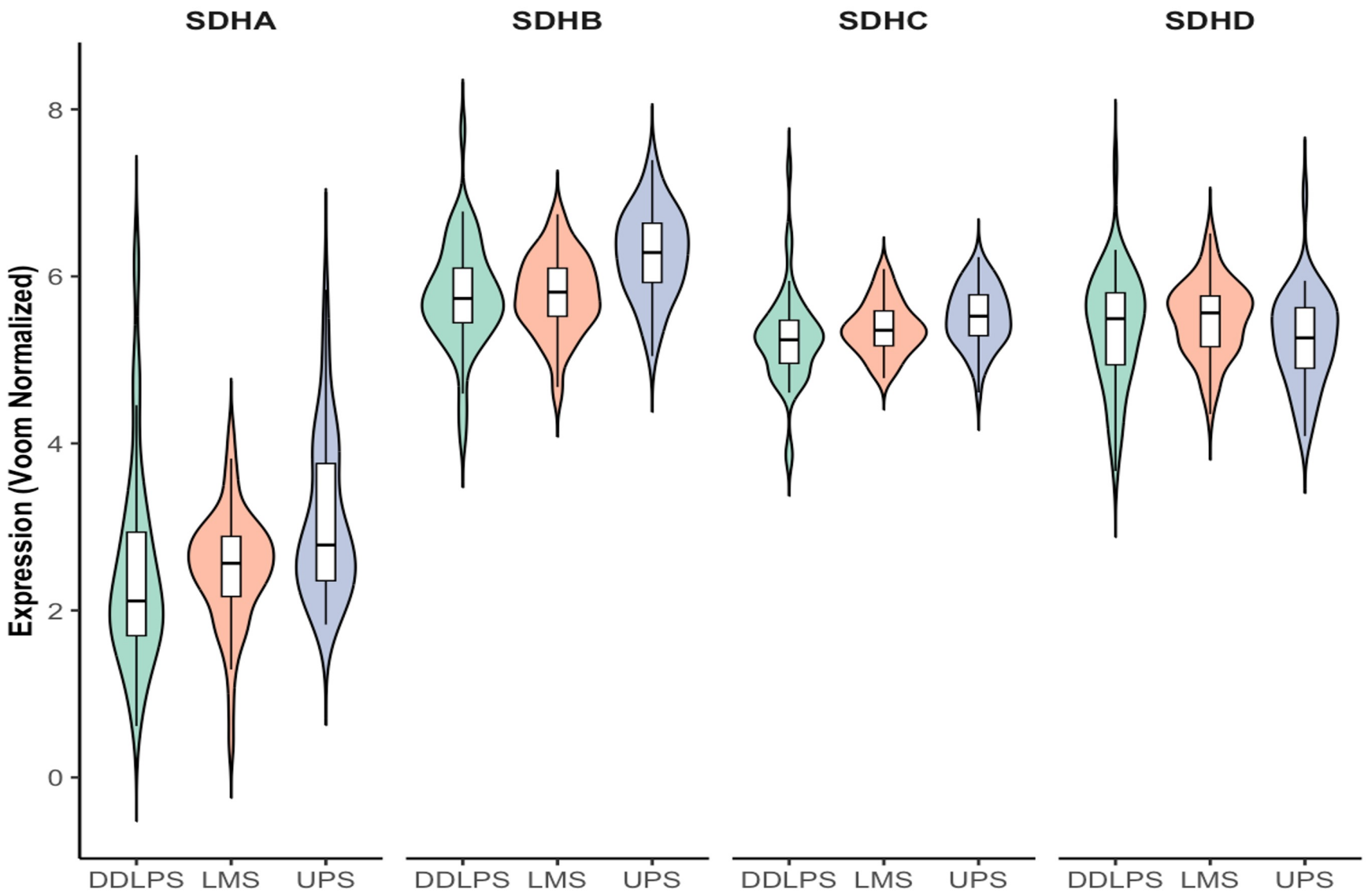

SDHA Differential Gene Expression

Comparison	adj_p_value	logfc
LMS VS DDLPS	0.813	-0.058
UPS vs LMS	0.015	0.593
UPS vs DDLPS	0.012	0.535

Note. Limma-Voom Differential expression results

SDHB Differential Gene Expression

Comparison	adj_p_value	logfc
LMS VS DDLPS	0.873	-0.022
UPS vs LMS	<0.001	0.501
UPS vs DDLPS	<0.001	0.479

Note. Limma-Voom Differential expression results

SDHC Differential Gene Expression

Comparison	adj_p_value	logfc
LMS VS DDLPS	0.164	-0.135
UPS vs LMS	0.016	0.271
UPS vs DDLPS	0.175	0.136

Note. Limma-Voom Differential expression results

SDHD Differential Gene Expression

Comparison	adj_p_value	logfc
LMS VS DDLPS	0.35	-0.124
UPS vs LMS	0.455	-0.128
UPS vs DDLPS	0.06	-0.251

Note. Limma-Voom Differential expression results

Figure 4

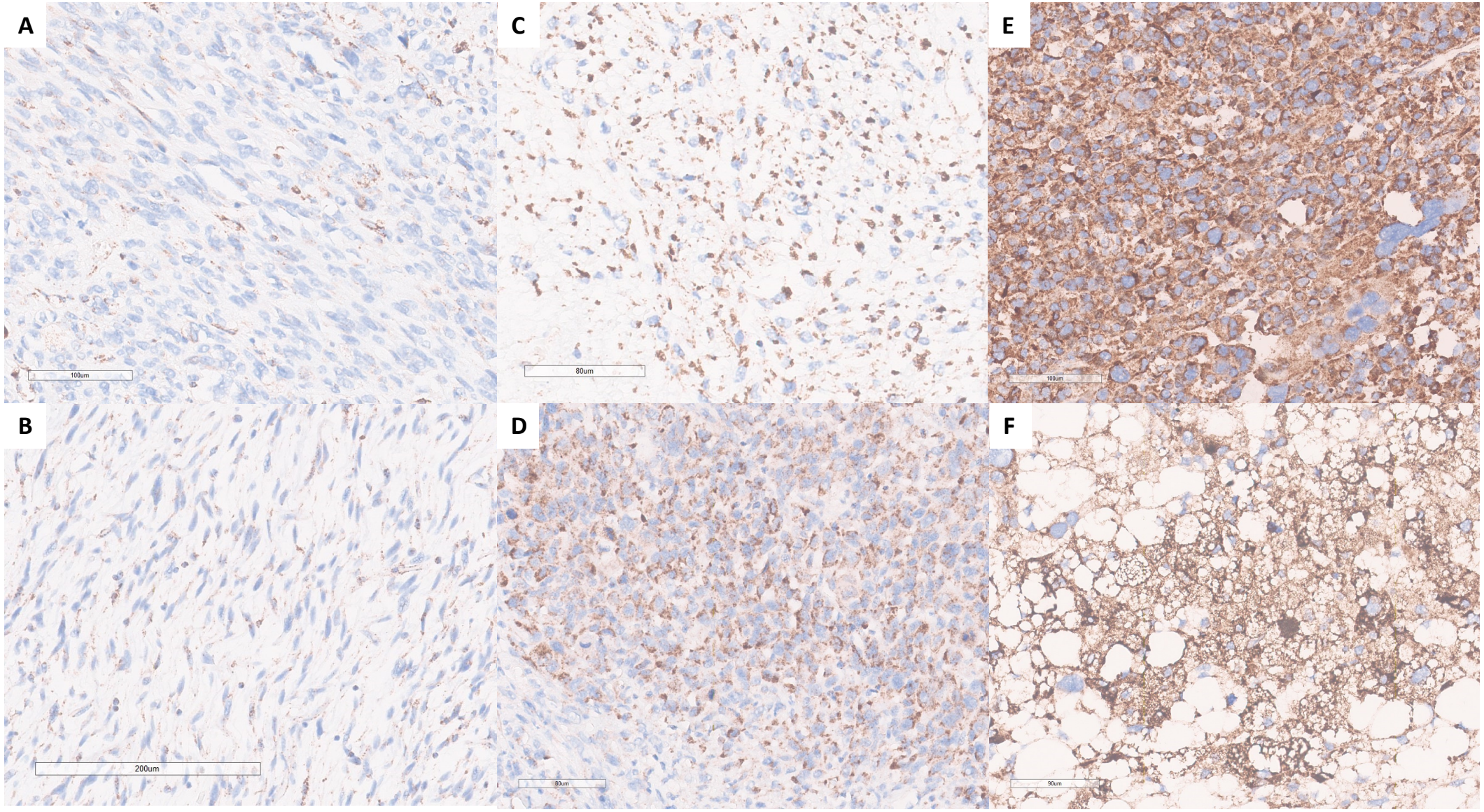

Figure 5

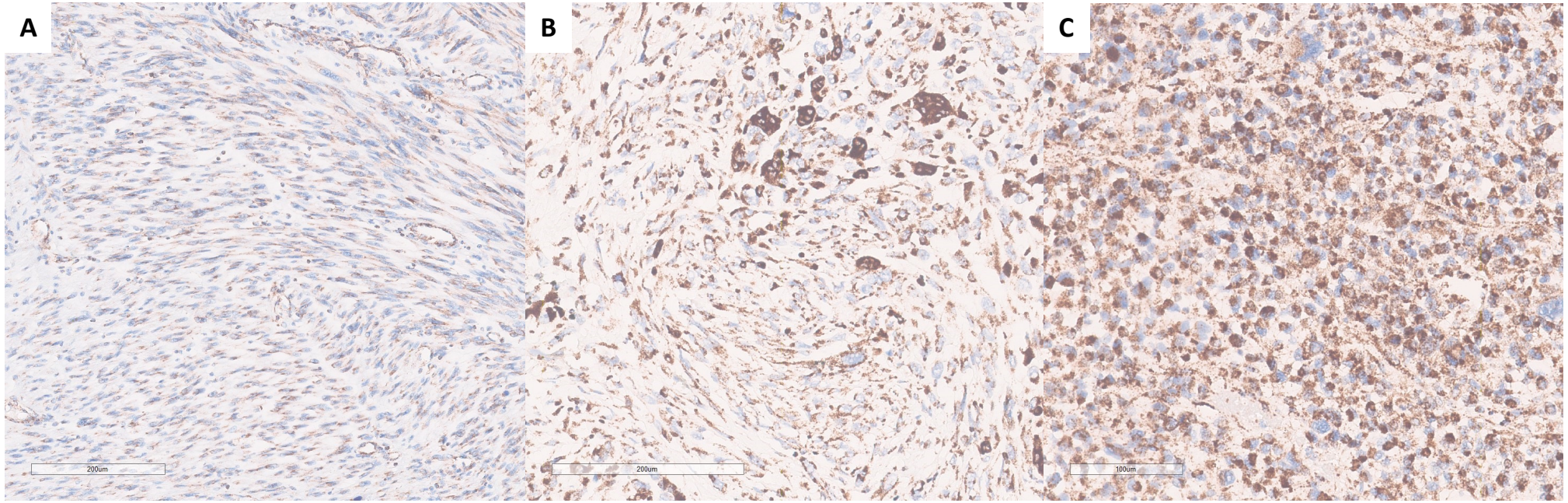

Figure 6

Figure 6a

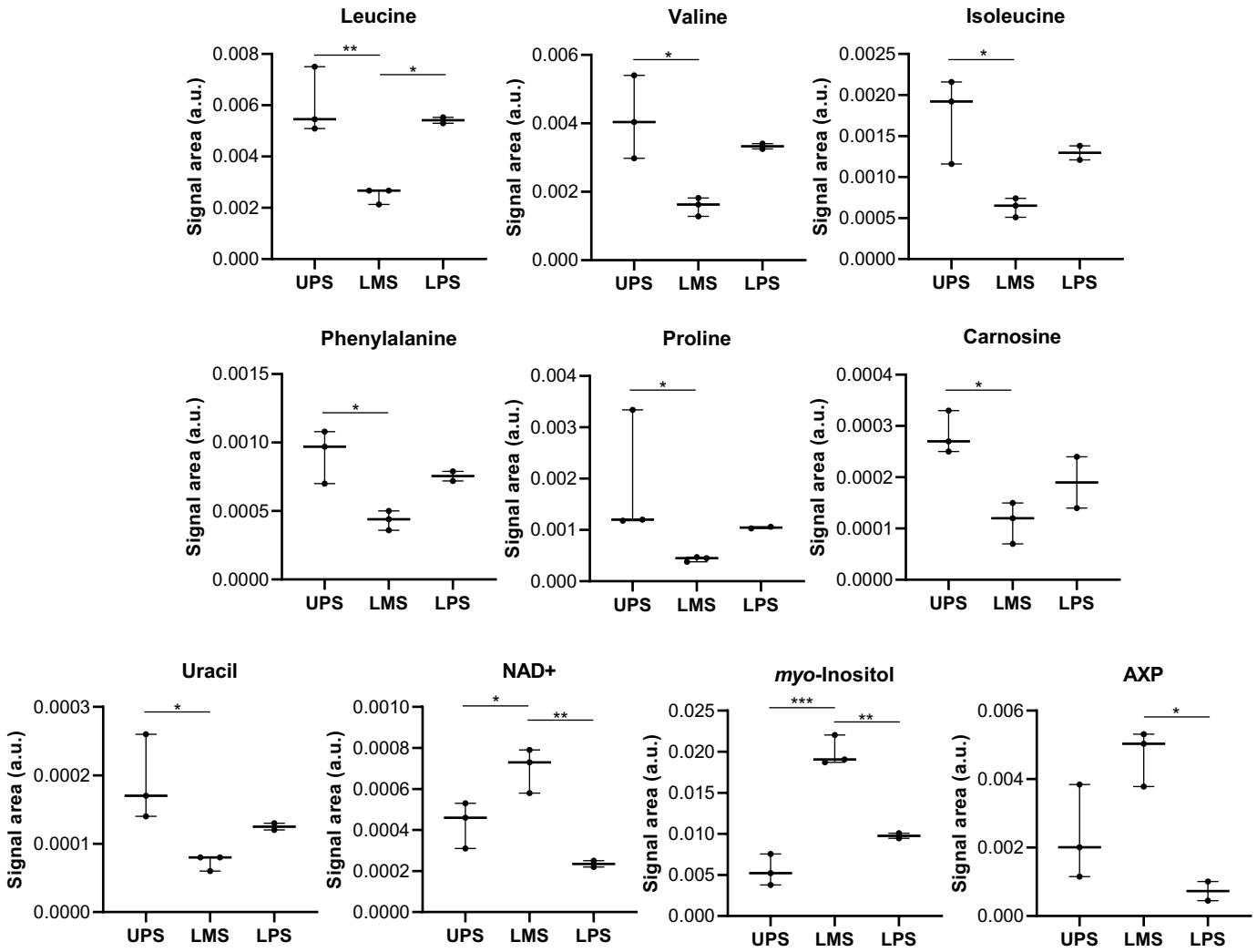

Figure 6
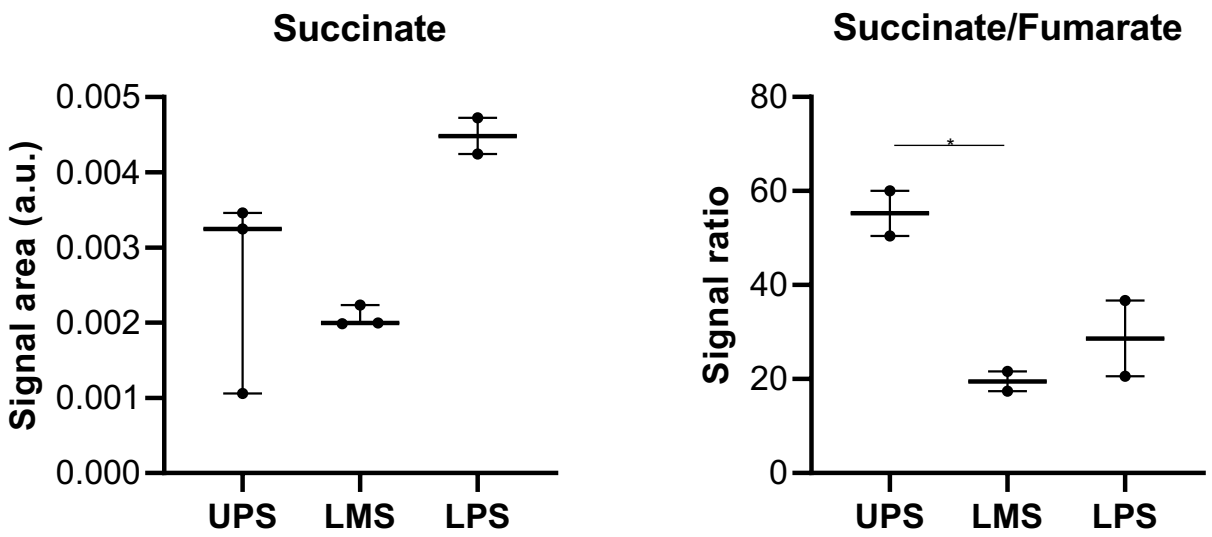
Figure 6b